

# Inverse Realized Laplace Transforms for Nonparametric Volatility Density Estimation in Jump-Diffusions\*

Viktor Todorov<sup>†</sup> and George Tauchen<sup>‡</sup>

September 27, 2011

## Abstract

We develop a nonparametric estimator of the stochastic volatility density of a discretely-observed Itô semimartingale in the setting of an increasing time span and finer mesh of the observation grid. There are two steps. The first is aggregating the high-frequency increments into the realized Laplace transform, which is a robust nonparametric estimate of the underlying volatility Laplace transform. The second step is using a regularized kernel to invert the realized Laplace transform. The two steps are relatively quick and easy to compute, so the nonparametric estimator is practicable. We derive bounds for the mean squared error of the estimator. The regularity conditions are sufficiently general to cover empirically important cases such as level jumps and possible dependencies between volatility moves and either diffusive or jump moves in the semimartingale. Monte Carlo work indicates that the nonparametric estimator is reliable and reasonably accurate in realistic estimation contexts. An empirical application to 5-minute data for three large-cap stocks, 1997-2010, reveals the importance of big short-term volatility spikes in generating high levels of stock price variability over and above that induced by price jumps. The application also shows how to trace out the dynamic response of the volatility density to both positive and negative jumps in the stock price.

**Keywords:** Laplace transform, stochastic volatility, ill-posed problems, regularization, nonparametric density estimation, high-frequency data.

**JEL classification:** C51, C52, G12.

---

\*Research partially supported by NSF Grant SES-0957330.

<sup>†</sup>Department of Finance, Kellogg School of Management, Northwestern University, Evanston, IL 60208; e-mail: v-todorov@northwestern.edu.

<sup>‡</sup>Department of Economics, Duke University, Durham, NC 27708; e-mail: george.tauchen@duke.edu.

# 1 Introduction

Continuous-time models are widely used in empirical finance to model the evolution of financial asset prices. Absence of arbitrage (under some technical conditions) implies that traded financial assets should be semimartingales and typically most, if not all, applications restrict attention to Itô semimartingales, i.e., semimartingales with characteristics absolutely continuous in time. Thus the standard asset pricing model for the log-financial price  $X_t$  is of the form

$$dX_t = \alpha_t dt + \sqrt{V_t} dW_t + dJ_t, \quad (1)$$

where  $\alpha_t$  and  $V_t > 0$  are processes with càdlàg paths,  $W_t$  is a Brownian motion,  $J_t$  is a jump process.

In Section 2 farther below we give the technical conditions for the components comprising  $X$  in (1), while here we briefly describe their main roles in determining the dynamics of the  $X$  process.  $\alpha_t$  captures risk premium (and possibly risk-free rate) and is well-known to be present but will not be the object of interest in this paper. As will be seen below, it gets filtered out in our estimation process. The jump component,  $J_t$ , highlighted by Barndorff-Nielsen and Shephard (2004), among others, accounts according to earlier empirical evidence typically for 5 to 15 percent of the total variance of the increments in  $X$ . Jumps reflect the fact that financial time series exhibit very sharp short-term moves incompatible with the continuous sample paths implied by diffusive models. Much of the evidence on jumps has been adduced using very high frequency data; earlier efforts using coarsely sampled (daily) data were at best mildly successful in handling both jumps and diffusive price moves. Similar to  $\alpha_t$ ,  $J_t$  will be filtered out in our analysis. The volatility term,  $V_t$ , represents the dominate component of the variance of increments in  $X$  and thus is most widely studied, see e.g., Mykland and Zhang (2009) and the many references therein. The volatility process is well known to be negatively correlated with the increments in the driving diffusion  $W_t$ . This negative correlation is the so called “leverage” effect, a term due to Black (1976), and the effect has been extensively documented in a wide variety of studies using various statistical methods. Of course, price and volatility can have dependence beyond the “leverage” effect as in the symmetric GARCH processes, e.g., Klüppelberg et al. (2004).

This paper develops a method to estimate nonparametrically from high-frequency data (by way of a Laplace transform) the marginal law of the stochastic volatility process  $V_t$  as well as its conditional law for certain interesting events. For reasons just described, we develop the density estimation method within a very general setting where  $V_t$  and  $W_t$  can be dependent and jumps and a drift term are present as well. Although the preceding discussion is for  $X$  being a financial asset

price, the results in this paper obviously apply to any statistical application where high-frequency observations of an Itô semimartingale (which includes many continuous-time models) are available.

On intuitive level, our method can be described as follows. We use a cosine transformation of appropriately re-scaled high-frequency returns data (which is akin to using a bounded influence function) that essentially separates out the jumps and the drift, thereby leaving (essentially) the diffusive piece scaled by  $\sqrt{V_t}$ . Averaging the transform over time yields the realized Laplace transform of volatility studied in Todorov and Tauchen (2011). This transform estimates the real-valued Laplace transform of the underlying spot volatility process, and it further achieves this without any need for staggering of price increments, explicit truncation, or other techniques involving tuning parameters commonly used for jump-robust measures of volatility.

Real Laplace transforms uniquely identify the distribution of nonnegative random variables, so a second step in the estimation is to invert the realized Laplace transform of volatility and thereby recover an estimate of the volatility density. The task of inverting real Laplace transforms also arise in analysis of certain physical phenomena. Historically, inversion of the real Laplace transform, where transform values are only available on the nonnegative real axis but not the entire complex plane, was among the most notorious of all ill-posed problems. However, recent regularization algorithms developed by Kryzhniy (2003a,b) along with the availability of high speed computing equipment (for nested numerical integrations) render the inversion a quick and easy task to compute in a matter of a few minutes using standard software like Matlab.

The role of regularization in this context is to guarantee statistical consistency when the volatility Laplace transform is recovered with sampling error, as is case here. The results in Todorov and Tauchen (2011) and Kryzhniy (2003a,b), when combined, imply the consistency of our density estimator. Here we go one step further and derive bounds on the size of the density estimation error due to regularization and estimation of the volatility Laplace transform, which in turn provides bounds on the rate of convergence of our density estimate. Although the method developed here is in a jump-diffusion setting, it can be easily extended to the setting where  $W_t$  in (1) is pure-jump martingale with a Lévy density that behaves like that of a stable process around zero. The only modification to the analysis in the current paper is in the way the volatility Laplace transform is recovered for which the small-scale behavior of the driving pure-jump martingale plays a central role; to keep the analysis simple we do not consider this extension here.

We can compare our method with the deconvolution approach of Van Es et al. (2003) and Comte and Genon-Catalot (2006). The methods of these papers are developed for a process without jumps, i.e., without  $J_t$  in (1), and with stochastic volatility  $V_t$  independent from the Brownian motion  $W_t$

in (1) (and further without drift in the case of Comte and Genon-Catalot (2006)). In such a setup, the logarithm of the squared price increments is (approximately) a sum of signal (the log volatility) and noise, and one can apply a deconvolution kernel (Van Es et al. (2003)) or a penalized projection (Comte and Genon-Catalot (2006)) to generate a nonparametric estimate of the distribution of the log volatility. The rate of convergence of this estimation depends, of course, on the smoothness of the volatility density, with a logarithmic rate in the least favorable situation. In our case, similar rates apply on comparable smoothness conditions for the density, but under the much weaker and empirically plausible assumptions on jumps and leverage for  $X$  in (1). On a more practical level, the method here avoids taking logarithms of high-frequency squared price increments, which could be problematic in some instances, because the log transformation inflates (despite the centering) the non-trivial number of zero returns due to discretization, and it further weighs more heavily the smaller increments which are more prone to microstructure noise effects.

We test our method on simulated data that mimics a typical data set available in finance and find that the method can recover reasonably well the volatility density. We further provide guidance on the choice of the regularization parameter.

In an empirical application, we investigate the distribution of the spot volatility for three large-cap stocks. Earlier work by Andersen et al. (2001) investigated the distribution of daily realized volatility (which is the sum of the squared daily high-frequency increments) of financial series, exchange rates in their case. Here we go one step further and recover the distribution of spot volatility. Spot and realized volatility differ due to the time-aggregation as well as the presence of price jumps. The evidence suggests that the density of spot volatility is less concentrated around the mode with more mass in the extreme tails than that of a (jump-robust) realized volatility measure. This latter finding underscores the importance of short-term volatility spikes. We also invert the realized Laplace transform on days following a significant price jump and provide non-parametric evidence that volatility increases significantly after jumps with diminishing impact over time. Overall, the nonparametric analysis sheds light on the importance of the variability of the stochastic volatility process  $V_t$  in accounting for big moves in asset prices in addition to pure price jumps generated by  $J_t$ .

The rest of the paper is organized as follows. Section 2 states the problem and the assumptions and presents the main asymptotic results. Section 3 reports numerical experiments on the inversion of real-valued Laplace transform using our proposed method, both in the case when the latter is the true transform and the case where it is recovered from high-frequency observations of a jump-diffusion process. Section 4 reports on the empirical application to high-frequency stock data.

Section 5 concludes. Section 6 contains the proof of the theoretical results.

## 2 Main results

We start with describing our estimation method and deriving its asymptotic behavior.

### 2.1 Setup and definitions

We first state the necessary assumptions that we will need. The observed process  $X$  is given by its dynamics specified in (1) and is defined on a filtered probability space  $(\Omega, \mathcal{F}, (\mathcal{F}_t)_{t \geq 0}, \mathbb{P})$ . Our assumption for  $X$  is given in the following.

**Assumption A.** *For the process  $X$  specified in (1) assume*

- A1.** For every  $t \geq 0$  we have  $\mathbb{E} \{ |\alpha_t|^2 + |V_t|^2 + |J_t|^2 \} \leq K$  for some positive constant  $K$ .
- A2.**  $J_t$  is a jump process of the form  $J_t = \int_0^t \int_{\mathbb{R}} \kappa(x) \tilde{\mu}(ds, dx) + \int_0^t \int_{\mathbb{R}} \kappa'(x) \mu(ds, dx)$  where  $\mu$  is integer-valued measure on  $\mathbb{R}_+ \times \mathbb{R}$  with compensator  $\nu(ds, dx)$ ;  $\tilde{\mu}(ds, dx) = \mu(ds, dx) - \nu(ds, dx)$ ;  $\kappa(x)$  is continuous function with  $\kappa(x) = x$  around zero and it is zero outside a compact set containing the zero;  $\kappa'(x) = x - \kappa(x)$ .
- A3.** For every  $t, s \geq 0$  we have  $\mathbb{E} (|V_t - V_s|^2 | \mathcal{F}_{s \wedge t}) \leq K_{s \wedge t} |t - s|$  for some  $\mathcal{F}_{s \wedge t}$ -adapted random variable  $K_{s \wedge t}$  with  $\mathbb{E} |K_{s \wedge t}|^{2+\iota} < K$  for some positive constant  $K$  and arbitrary small  $\iota > 0$ , and  $\mathbb{E} |J_t - J_s|^p \leq K |t - s|$  for every  $p \in (\beta, 2]$ , some  $\beta \in [0, 2)$  and a positive constant  $K$ .
- A4.**  $V_t$  is a stationary and  $\alpha$ -mixing process with  $\alpha_t^{\text{mix}} = O(t^{-1-\iota})$  when  $t \rightarrow \infty$  for some arbitrary small  $\iota > 0$ , where

$$\alpha_t^{\text{mix}} = \sup_{A \in \mathcal{F}_0, B \in \mathcal{F}^t} |\mathbb{P}(A \cap B) - \mathbb{P}(A)\mathbb{P}(B)|, \quad \mathcal{F}_0 = \sigma(V_s, s \leq 0) \text{ and } \mathcal{F}^t = \sigma(V_s, s \geq t). \quad (2)$$

Assumption A1 imposes some mild integrability conditions on the different components of  $X$ . Some of them can be potentially relaxed, but nevertheless they are very weak and satisfied in virtually all parametric models used in empirical finance. Assumption A2 specifies the jump process in  $X_t$ . We note that there is very little structure that is assumed for the jumps and in particular time-variation in the jump intensity (both in the form of time-varying jump size and time-varying jump intensity) is allowed for. In assumption A3 we impose restriction on the variability in the processes  $V_t$  and  $J_t$ . The part of A3 concerning  $V_t$  is very minimal and in particular is satisfied when  $V_t$  is an Itô semimartingale (as is the case in the popular affine jump-diffusion framework) but it also holds for certain long-memory specifications (A3 also strengthens slightly the integrability condition for

$V_t$  in A1). We also point out that assumption A allows for jumps in  $V_t$  that can have arbitrary dependence with  $J_t$  which will be of practical importance as we will see in the empirical application. The restriction of A3 on the jump component  $J_t$  is that the so-called Blumenthal-Gettoor index of the latter (which can be random) is bounded by  $\beta$ . We note that we allow for  $\beta > 1$  which means that infinite variation jumps are included in our analysis as well. Finally A4 is a (standard) mixing condition on the volatility process and it is satisfied in wide classes of volatility models.

As stated already in the introduction, our goal in this paper is to recover nonparametrically the density of the spot volatility marginal law (with respect to Lebesgue measure), which we denote with  $f(x)$  (and assume to exist almost everywhere). Our next assumption imposes the necessary conditions on  $f(x)$ .

**Assumption B.** *The marginal law of  $V_t$  has density  $f(x)$  which is piecewise continuous and has piecewise continuous derivatives. We further have*

**B1.**  *$f'(x) = O(x^{-q})$  as  $x \rightarrow 0$  for some nonnegative  $q < 5/2$ .*

**B2.**  *$f(x)$  and  $f'(x)$  are bounded on  $\mathbb{R}^+$  with  $f(x) = o(x^{-1-\iota})$  and  $f'(x) = o(x^{-2-\iota})$  for some arbitrary small  $\iota > 0$  when  $x \rightarrow \infty$  and  $f(0+) = 0$ .*

The degree of smoothness of the density naturally impacts the precision of estimation as in standard nonparametric density estimation (based on direct observations of the process) and the above assumption provides such conditions. Assumption B1 is quite weak and allows for the density of  $V_t$  to explode around zero. Assumption B2 strengthens B1 by ruling out explosions around zero and further requiring a rate of decay of the volatility density (and its derivative) at infinity.

Our strategy of estimating nonparametrically the volatility density from high-frequency observations of  $X_t$  is based on first recovering the Laplace transform of the volatility and then inverting it. To this end, we denote the *real-valued* Laplace transform of the marginal distribution of the process  $V_t$  with

$$\mathcal{L}(u) = \mathbb{E} \left( e^{-uV_t} \right), \quad u \geq 0. \quad (3)$$

In Todorov and Tauchen (2011) we have proposed the following nonparametric estimate of the unobserved volatility Laplace transform from high-frequency observation of  $X_t$  on the discrete grid  $0, \frac{1}{n}, \dots, \frac{j}{n}, \dots, T$

$$\widehat{\mathcal{L}}(u) = \frac{1}{nT} \sum_{i=1}^{nT} \cos \left( \sqrt{2un} \Delta_i^n X \right), \quad \Delta_i^n X = X_{\frac{i}{n}} - X_{\frac{i-1}{n}}, \quad u \geq 0, \quad (4)$$

which we refer to as realized Laplace transform.

As shown in Todorov and Tauchen (2011), for  $T \rightarrow \infty$  and  $n \rightarrow \infty$ , we have locally uniformly in  $u$

$$\widehat{\mathcal{L}}(u) \xrightarrow{\mathbb{P}} \mathcal{L}(u), \quad (5)$$

and there is an associated Central Limit theorem but we will not make use of it here. We note, in particular, that  $\widehat{\mathcal{L}}(u)$  is robust to presence of jumps in  $X$  (the component  $J_t$  in (1)) as well as any dependence between the volatility process  $V_t$  and the Brownian motion  $W_t$ .

The (real-valued) Laplace transform of a nonnegative random variable uniquely identifies its distribution (see e.g., Feller (1971)). However recovering the distribution from the Laplace transform is an ill-posed problem (Tikhonov and Arsenin (1977)) and hence one needs a regularization to make the inversion problem a continuous operator on the space of Laplace transforms. Here, we adopt an approach proposed in Kryzhniy (2003a,b) and propose the following regularized inversion of the true Laplace transform  $\mathcal{L}(u)$

$$f_R(x) = \int_0^\infty \mathcal{L}(u) \Pi(R, xu) du, \quad (6)$$

where  $R > 0$  is a regularization parameter and the kernel  $\Pi(R, x)$  is defined as

$$\begin{aligned} \Pi(R, x) = \frac{4}{\sqrt{2}\pi^2} & \left[ \sinh\left(\frac{\pi R}{2}\right) \int_0^\infty \frac{\sqrt{u} \cos(R \ln(u))}{u^2 + 1} \sin(xu) du \right. \\ & \left. + \cosh\left(\frac{\pi R}{2}\right) \int_0^\infty \frac{\sqrt{u} \sin(R \ln(u))}{u^2 + 1} \sin(xu) du \right]. \end{aligned} \quad (7)$$

As shown in Kryzhniy (2003a),  $f_R(x) \rightarrow \frac{f(x-) + f(x+)}{2}$  for every  $x > 0$  (pointwise) as  $R \rightarrow \infty$  where we define  $f(x+) = \lim_{y \downarrow x} f(y)$  and  $f(x-) = \lim_{y \uparrow x} f(y)$ . We further have

$$\left| \int_0^\infty (\mathcal{L}_1(u) - \mathcal{L}_2(u)) \Pi(R, xu) du \right| \leq K \sup_{u \in \mathbb{R}_+} |\mathcal{L}_1(u) - \mathcal{L}_2(u)|,$$

for any two Laplace transforms  $\mathcal{L}_1(u)$  and  $\mathcal{L}_2(u)$  (Kryzhniy (2003a), Theorem 2) and a positive constant  $K$ , which shows that this is indeed a regularization of the ill-posed inversion problem (Tikhonov and Arsenin (1977)).

It is easy to develop intuition about the regularization by using the connection between the regularized and true density derived in Kryzhniy (2003a)

$$f_R(x) = \int_0^\infty f(u) \delta_{R,x}(u) du, \quad \delta_{R,x}(u) = \frac{2 \coth(\pi R) \sqrt{ux}}{\pi(u^2 - x^2)} \sin(R \ln(u/x)), \quad x > 0. \quad (8)$$

The function  $\delta_{R,x}(u)$  is a smooth approximation of the Dirac delta function at the point  $x$ . The regularization parameter  $R$  determines the degree of smoothing and corresponds to the choice of the bandwidth in regular nonparametric kernel estimators where one has direct observations of the

variable of interest (unlike here where we do not observe directly  $V_t$ ). Higher values of  $R$  means that  $\delta_{R,x}(u)$  is closer to the Dirac delta and hence this implies less smoothing. However, these higher values can lead to a good result only if the precision of the input (here the realized Laplace transform) is high, otherwise the oscillations in  $\delta_{R,x}(u)$  will cause very noisy density estimates. Exactly the opposite holds for low values of  $R$ . This is further confirmed from Figure 1 where we plot the function  $\delta_{R,x}(u)$  for several different values of  $x$  and a low and a high value of  $R$  that we will actually use in our numerical work later on.

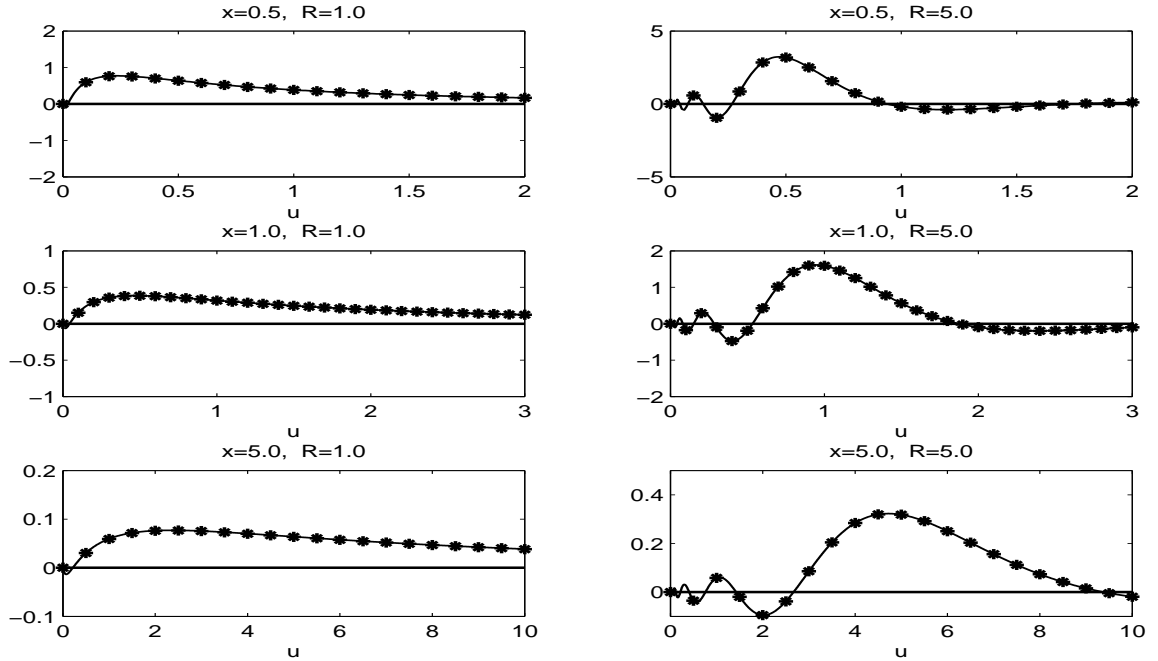


Figure 1: *The function  $\delta_{R,x}(u)$ .* The solid lines correspond to the theoretical value of  $\delta_{R,x}(u)$  given in (8). The dots on the plots correspond to our numerical evaluation of  $\delta_{R,x}(u)$  via evaluating the integral in (6) with  $\mathcal{L}(u) = \exp(-u * x)$ .

An alternative representation of  $\delta_{R,x}(u)$  is as the regularized inverse of the function  $\exp(-u * x)$ , that is  $\delta_{R,x}(u) = \int_0^\infty \exp(-t * x) \Pi(R, u * t) dt$ . We can use this connection to check the impact on the estimation of the error due to the numerical integration involved in computing (6) and (7). We plot the resulting estimates of  $\delta_{R,x}(u)$  with the dotted lines on Figure 1. As seen from the figure, the dotted lines plot on the top of the solid lines (which correspond to the theoretical value of  $\delta_{R,x}(u)$  in (8)) which indicates that numerical error is negligible for the values of  $R$  used in the computations (which covers the range of  $R$  that we are going to use in practice).

The feasible analogue of  $f_R(x)$ , based on the realized Laplace transform, is naturally defined as

$$\widehat{f}_R(x) = \int_0^\infty \widehat{\mathcal{L}}(u)\Pi(R, xu)du, \quad (9)$$

and this will be our nonparametric estimate of the density of  $V_t$  from the discrete observations of the underlying process  $X_0, X_{\frac{1}{n}}, \dots, X_T$ . We next turn to analysis of the asymptotic properties of our estimator  $\widehat{f}_R(x)$  defined in (9).

## 2.2 Inversion of Real-Valued Laplace Transforms

We have the following asymptotic result for the regularized estimated density  $\widehat{f}_R(x)$ .

**Theorem 1** *For the process  $X$  in (1), we assume that assumption A holds and denote  $\widetilde{f}(x) = \frac{f(x^-)+f(x^+)}{2}$ . Let  $n \rightarrow \infty$ ,  $T \rightarrow \infty$  and  $R \rightarrow \infty$ .*

(a) *If assumption B1 holds then*

$$\left(f_R(x) - \widetilde{f}(x)\right)^2 = O\left(R^{-2\left(\frac{5-2q}{3} \wedge 1\right)} \times \log^2(R)\right), \quad (10)$$

$$\begin{aligned} \mathbb{E}\left(\widehat{f}_R(x) - f_R(x)\right) &= O\left(e^{\pi R/2} R^2 \left(T^{-1/2} + n^{-((1/\beta) \wedge 1 - \beta/2 - \iota) \wedge 1/4}\right)\right), \\ \mathbb{E}\left(\widehat{f}_R(x) - f_R(x)\right)^2 &= O\left(e^{\pi R} R^4 \left(T^{-1} + n^{-(1/2) \wedge (1-\beta/2) + \iota}\right)\right), \quad \forall \iota > 0. \end{aligned} \quad (11)$$

(b) *If assumption B2 holds then*

$$\mathbb{E}\left\{\int_{\mathbb{R}_+} w(x) \left(\widehat{f}_R(x) - \widetilde{f}(x)\right)^2 dx\right\} = O\left(\frac{\log^2(R)}{R^2} \sqrt{e^{\pi R} R^4 \left(T^{-1} + n^{-1+\beta/2+\iota}\right)}\right), \quad \forall \iota > 0, \quad (12)$$

where  $w(x)$  is a bounded nonnegative-valued function with  $w(x) = o(x^2)$  for  $x \rightarrow 0$ .

If further we denote

$$\widetilde{f}_R(x) = \int_0^\infty \mathcal{L}(u)\widetilde{\Pi}(R, xu)du, \quad \widetilde{\Pi}(R, xu) = \chi(R^2 x)\Pi(R, xu), \quad \chi(u) = u \wedge 1, \quad (13)$$

then (under assumption B2)

$$\mathbb{E}\left\{\int_{\mathbb{R}_+} \left(\widetilde{f}_R(x) - \widetilde{f}(x)\right)^2 dx\right\} = O\left(\frac{\log^2(R)}{R^2} \sqrt{e^{\pi R} R^8 \left(T^{-1} + n^{-1+\beta/2+\iota}\right)}\right), \quad \forall \iota > 0. \quad (14)$$

The result of Theorem 1 implies that  $\widehat{f}_R(x)$  is a consistent estimate of the volatility density  $f(x)$  at the points of continuity of the latter and estimates the average of the right and left limits (which exist by assumption B) at the points of discontinuity. The theorem goes one step further and provides bounds on the bias and the variance of the estimator. There are two sources of bias in the

estimation. One, that is deterministic, arises from the regularization of the inversion, and naturally depends only on the regularization parameter  $R$ . Its bound is given in (10). The second source of bias is stochastic and arises from the discretization error, i.e., we do not observe directly the empirical volatility Laplace transform  $\frac{1}{T} \int_0^T e^{-uV_s} ds$  but we need to recover it from high-frequency data. The magnitude of this bias is given by the first expression in (11) and naturally depends only on the mesh of the observation grid, i.e.,  $1/n$ . Finally, the bound on the variance of the estimator is given in the second expression in (11). It depends both on the span of the data and the mesh of the observation grid. Its leading component (provided  $n$  is increasing sufficiently fast relative to  $T$ ) is given by

$$\frac{1}{T} \int_0^\infty \int_0^\infty \int_0^\infty \Pi(R, xu) \Pi(R, xv) \Sigma_{u,v} du dv dx,$$

where  $\Sigma_{u,v}$  is the long-run variance-covariance kernel of  $\frac{1}{T} \int_0^T (e^{-uV_s} - \mathcal{L}(u)) ds$ .

In the most common case of assumption B2 and provided  $n \propto T^\alpha$  for some  $\alpha > 0$ , we can set  $R = \gamma \frac{\log(T)}{\pi}$  for some positive  $\gamma < \alpha(1 - \beta/2) \wedge 1$ , and get the squared bias and the variance of the estimator of (almost) the same order of magnitude. Such choice of  $R$  will result in (only) logarithmic rate of convergence for our volatility density estimator. This is not surprising given our weak assumption B for the density  $f(x)$ . Squared logarithmic rate of convergence for the log-volatility density, in a setting where  $X_t$  does not contain jumps and  $V_t$  is independent from  $W_t$ , is obtained via a deconvolution approach in Van Es et al. (2003) where it is connected with the optimal rate of deconvoluting a density in the presence of super-smooth noise derived in Fan (1991) (in the context of i.i.d. data). Van Es et al. (2003) assume  $f(x)$  is twice continuously differentiable and obtain optimal rate of convergence for their density estimator of squared logarithmic rate while here we assume only first-order derivatives for  $f(x)$  and hence we end up with (almost) logarithmic rate of convergence (which is the optimal deconvolution rate under this smoothness assumption for  $f(x)$  in the presence of super-smooth noise, see Fan (1991)).

Similarly, here if we assume more smoothness conditions for the volatility density  $f(x)$  we can show that the deterministic bias due to the regularization  $f(x) - f_R(x)$  is of smaller order of magnitude than the bound given in (10). This in turn will imply faster rate of convergence for our volatility density estimator (provided  $R$  is chosen optimally). Thus we have a natural link between the rate of convergence of our density estimator and the degree of smoothness of the unknown volatility density. This is similar to the results in Comte and Genon-Catalot (2006). In the setting of no drift and no jumps as well as independent  $W_t$  and  $V_t$ , Comte and Genon-Catalot (2006) show that a penalized projection type volatility density estimator can provide faster rates of convergence for smoother volatility densities.

Under the minimal smoothness requirement for the volatility density in assumption B, the relative speed condition between  $T$  and  $n$  is relatively weak, i.e., as pointed above it is of the form  $n \propto T^\alpha$  for some  $\alpha > 0$ . Such a condition, in particular, is much weaker than the corresponding requirement in the problem of parametric estimation of diffusions from discrete observations, see e.g., Prakasa Rao (1988). This of course is no surprise and is a mere reflection of the much smaller role (in relative terms) played by the discretization error in our nonparametric volatility density estimation. We also point out that, quite naturally, the discretization error is bigger, the bigger is the bound on the activity index of jumps in  $X$ ,  $\beta$ . This is because higher activity jumps become harder to separate from diffusive innovations in the increments of  $X$ . We also point out that the discretization error is of smaller magnitude in (12) versus (11) (provided  $\beta < 1$ ) because of the extra assumption on the behavior of the volatility density around zero in assumption B2 (the volatility density approaches zero around the origin).

We note further that the result in part (a) is pointwise, i.e., for fixed  $x$ , while that in part (b) is for the mean integrated squared error (note that under B1,  $f(x)$  does not need to belong to  $L^2(\mathbb{R})$ ). For the estimator  $\widehat{f}_R(x)$ , we provide in (12) a bound for its mean integrated squared error weighted by a function  $w(x)$  that is bounded and  $o(x^2)$  as  $x \rightarrow 0$  but is otherwise arbitrary. The role of  $w(x)$  is to down-weight the estimation error in  $\widehat{f}_R(x)$  around zero. In (13) we propose a slight modification of  $\widehat{f}_R(x)$  which we define as  $\widetilde{f}_R(x)$ . We have  $\widetilde{f}_R(x) = \chi(R^2x)\widehat{f}_R(x)$  and the function  $\chi(R^2x)$  serves to dampen our original density estimate around zero. This dampening in turn allows us to bound in (14) the mean integrated squared error of  $\widetilde{f}_R(x)$  with  $w(x) = 1$ , i.e., without any down-weighting of the estimation error around zero. In our applications below we will use  $\widehat{f}_R(x)$  but we will evaluate it starting from sufficiently small value that is above zero, guidance for which can be easily obtained from the quantiles of any nonparametric daily integrated volatility estimates.

Finally, the analysis here can be easily extended to recovering the volatility density conditioned on some set. One interesting example, that we will consider in our empirical application, is the occurrence of big price jumps. The analysis in Bollerslev and Todorov (2011) can be used to bound the discretization error in identifying the set of big jumps (under some conditions for  $J_t$ ). Also, one can consider a setting of fixed span, i.e.,  $T$  fixed, in which  $\widehat{f}_R(x)$  will recover the density of the empirical volatility distribution over the given interval of time. Of course, for this we will need the smoothness assumption B to hold for the empirical volatility distribution. An example where this will be the case is when  $V_t$  is a non-Gaussian OU (Ornstein-Uhlenbeck) process (see equation (20) below) in which the driving Lévy process is compound Poisson (note that assumption B allows

for discontinuities in the density). Such models for volatility have been considered for example in Barndorff-Nielsen and Shephard (2001).

### 3 Numerical Experiments

We proceed next with numerical experiments to test our estimation method developed in the previous section. We first investigate how well our estimator can recover the volatility density in the infeasible scenario when the volatility Laplace transform is measured without error. We then consider the feasible scenario where the volatility Laplace transform is recovered from high-frequency price data via the realized Laplace transform.

#### 3.1 Inverting Known Laplace Transforms

We use two distributions in our numerical analysis here which will be the marginal laws of two popular volatility specifications that we will use in our Monte Carlo analysis below. The first is the Gamma distribution. We denote  $Y \sim G(a, b)$  for a random variable with probability density

$$f^G(x) = \frac{b^a x^{a-1}}{\Gamma(a)} e^{-bx} 1_{\{x>0\}}, \quad a, b > 0, \quad (15)$$

with corresponding real-valued Laplace transform given by

$$\mathcal{L}^G(u) = \left( \frac{1}{1 + u/b} \right)^a. \quad (16)$$

The second distribution we use here is the Inverse-Gaussian. We denote  $Y \sim IG(\mu, \nu)$  for a variable with probability density given by

$$f^{IG}(x) = \sqrt{\frac{\nu}{2\pi x^3}} \exp \left[ -\frac{\nu}{2\mu^2 x} (x - \mu)^2 \right] 1_{\{x>0\}}, \quad (17)$$

with corresponding real-valued Laplace transform

$$\mathcal{L}^{IG}(u) = \exp \left\{ (\nu/\mu) \left[ 1 - \sqrt{1 + 2\mu^2 u/\nu} \right] \right\}. \quad (18)$$

It is easy to check that the two distributions satisfy assumption B2. In Table 1 we list all the different cases considered in this section and give the corresponding parameters. We look in particular at settings with small, average, and big dispersion around the mode of the density. In Table 2 we report the Integrated Squared Error (ISE) in recovering the volatility density from the exact Laplace transform (over the quantile range  $Q_{0.005}$ - $Q_{0.995}$ ). The precision across all cases is very high. When we use the exact Laplace transform, there is obviously no estimation error and all error is due to the regularization and the numerical integration. We consider a range of values for the regularization

Table 1: Parameter Setting for the Monte Carlo

Case	Marginal Distribution of $V_t$	Parameter Values
<b>G-L</b>	Gamma	$\kappa = 0.02, \theta = 1.0, \sigma^2 = \frac{2\kappa\theta}{4.0}$
<b>G-M</b>	Gamma	$\kappa = 0.02, \theta = 1.0, \sigma^2 = \frac{2\kappa\theta}{2.5}$
<b>G-H</b>	Gamma	$\kappa = 0.02, \theta = 1.0, \sigma^2 = \frac{2\kappa\theta}{1.5}$
<b>IG-L</b>	Inverse-Gaussian	$\kappa = 0.02, \mu = 1.0, \nu = 3.0$
<b>IG-M</b>	Inverse-Gaussian	$\kappa = 0.02, \mu = 1.0, \nu = 1.0$
<b>IG-H</b>	Inverse-Gaussian	$\kappa = 0.02, \mu = 1.0, \nu = 0.5$

*Note:* Cases **G-L**, **G-M** and **G-H** correspond to the square-root diffusion process in (19) and the parameters of the Gamma distribution are given by  $a = \frac{2\kappa\theta}{\sigma^2}$  and  $b = \frac{2\kappa}{\sigma^2}$ . Cases **IG-L**, **IG-M** and **IG-H** correspond to the non-Gaussian OU process in (19) with Inverse-Gaussian marginal distribution.

parameter  $R$  and we can see from Table 2 that  $R$  plays a big role in the precision of the estimation. There is a pronounced U-shape pattern where small values of  $R$  result in bias due to over-smoothing (recall Figure 1) while very big values in  $R$  result in a bigger error due to the numerical integration. We also point out that the optimal value of  $R$  depends on the volatility density which is of course unknown.

### 3.2 Inverting Estimated Laplace Transforms

We turn next to the feasible case where the volatility density is not known and has to be estimated from high-frequency observations of  $X$ . We will consider two volatility specifications, widely used in empirical finance, whose marginal laws correspond to the Gamma and Inverse Gaussian distributions. The first is the square-root diffusion process given by

$$dV_t = \kappa(\theta - V_t)dt + \sigma\sqrt{V_t}dB_t, \quad \kappa, \sigma, \theta > 0, \quad \sigma \leq \sqrt{2\kappa\theta}. \quad (19)$$

The marginal distribution of the square-root diffusion process is the Gamma distribution with parameters  $a = \frac{2\kappa\theta}{\sigma^2}$  and  $b = \frac{2\kappa}{\sigma^2}$  in the parametrization of the previous subsection.

The second volatility specification is a non-Gaussian OU process given by

$$dV_t = -\kappa V_t dt + dL_t, \quad \kappa > 0, \quad (20)$$

where  $L_t$  is a Lévy subordinator. Following Barndorff-Nielsen and Shephard (2001), we specify the non-Gaussian OU process via its marginal distribution which will be the Inverse-Gaussian (which

Table 2: Integrated Squared Error of Density Estimate: Known Laplace Transform

Case	$\int_{\mathbb{R}} f^2(x) dx$	Regularization Paramater			
		$R = 2.0$	$R = 3.0$	$R = 4.0$	$R = 5.0$
<b>G-L</b>	0.6247	$5.40 \times 10^{-2}$	$1.11 \times 10^{-2}$	$1.60 \times 10^{-3}$	$1.92 \times 10^{-4}$
<b>G-M</b>	0.5301	$1.83 \times 10^{-2}$	$2.10 \times 10^{-3}$	$2.32 \times 10^{-4}$	$8.65 \times 10^{-4}$
<b>G-H</b>	0.4765	$4.10 \times 10^{-3}$	$3.90 \times 10^{-3}$	$6.99 \times 10^{-2}$	$1.21 \times 10^{-0}$
<b>IG-L</b>	0.6518	$5.01 \times 10^{-2}$	$8.10 \times 10^{-3}$	$1.10 \times 10^{-3}$	$2.89 \times 10^{-5}$
<b>IG-M</b>	0.5959	$8.40 \times 10^{-3}$	$4.68 \times 10^{-4}$	$2.31 \times 10^{-5}$	$1.56 \times 10^{-6}$
<b>IG-H</b>	0.6911	$5.30 \times 10^{-3}$	$2.74 \times 10^{-4}$	$5.15 \times 10^{-6}$	$3.28 \times 10^{-4}$

*Note:* The ISE  $\int_{Q_{0.005}^{0.995}} (f_R(x) - f(x))^2 dx$  is approximated by a Riemann sum with length of the discretization interval of 0.005. The range of integration is  $Q_{0.005}$ - $Q_{0.995}$  for  $Q_\alpha$  denoting the  $\alpha$ -quantile. Each of the cases is explained in Table 1.

is self-decomposable and hence this is possible, see e.g., Sato (1999)) with parametrization given in the previous subsection. It can be shown, see e.g., Todorov et al. (2011), that the Lévy measure of  $L_t$  is given by  $\frac{\kappa\nu e^{-\nu^2 x/(2\mu^2)}}{\sqrt{2}\Gamma(0.5)} \left[ \frac{x^{-1.5}}{2} + \frac{\nu^2 x^{-0.5}}{2\mu^2} \right]$ . Further, both volatility specifications in (19) and (20) satisfy assumption A. In Table 1 we report the parameter values in the different cases.

In the simulations, the price process is given by (1) with  $\alpha_t = 0$ ,  $J_t$  being a compound Poisson process with intensity 1/3 (i.e., one jump every three days on average) and normally distributed jump size with mean 0 and variance of 0.3 and one of the volatility specifications in (19) and (20). For simplicity in the Monte Carlo setup we set the volatility process independent from the price process. Simulation evidence in Todorov et al. (2011) indicates that the leverage effect has negligible effect on the realized Laplace transform in finite samples (recall from (5) that leverage has no asymptotic effect on  $\widehat{L}(u)$ ). In all experiments we set  $\mathbb{E}(V_t) = 1$  which implies jumps contribute approximately 10% of price variation, consistent with prior empirical evidence.

The unit of time in our simulation design is a day and we assume the span is  $T = 3,000$  days with  $n = 76$  which corresponds to sampling the price process every 5-minutes in a 6.5 hour trading day for approximately 12 years. In Table 3 we report the precision in recovering the volatility density from a single simulation from each of the scenarios for a range of values of the regularization parameter  $R$ . Comparing Table 2 with Table 3, not surprisingly, we can see that the ISE is orders of magnitude higher when Laplace transform has to be estimated from the data due to the estimation error. Nevertheless, provided the appropriate  $R$  is used, the error in estimation is

Table 3: Integrated Squared Error of Density Estimate: Estimated Laplace Transform

Case	$\int_{\mathbb{R}} f^2(x)dx$	Regularization Paramater			
		$R = 1.0$	$R = 1.5$	$R = 2.0$	$R = 3.0$
<b>G-L</b>	0.6247	0.1882	0.1003	0.0488	0.0128
<b>G-M</b>	0.5301	0.1066	0.0437	0.0162	0.0066
<b>G-H</b>	0.4765	0.0482	0.0161	0.0102	0.0677
<b>IG-L</b>	0.6518	0.2310	0.1390	0.0900	0.0840
<b>IG-M</b>	0.5959	0.1130	0.0432	0.0163	0.0099
<b>IG-H</b>	0.6911	0.0838	0.0268	0.0326	0.2980

*Note:* The computations are based on a single simulation from the models given in Table 1 and volatility Laplace transform estimate using the realized Laplace transform  $\widehat{L}(u)$  defined in (4). The ISE is approximated the same way as in the calculations for Table 2.

reasonably small. The values of  $R$  for which the precision is highest in the case of estimated Laplace transform are lower than the case when Laplace transform is known. This is because estimation error prevents us from using kernels with high “focusing” ability, i.e., we need to smooth more to remove the effect of the estimation error.

In the case of estimated Laplace transforms we have also a U-shaped pattern in the ISE: too large and too small values of  $R$  correspond to bigger ISE. This effect can be most clearly seen from Figure 2 where we plot the estimated densities for three different values of  $R$  for the simulation scenario G-H. Too low  $R$  results in over-smoothing and relatively big estimation bias. Increasing  $R$  improves the precision. However, when  $R$  is too big the estimation noise gets “blown up” and this leads to the oscillations in the estimated density (“inherited” from the more focused kernel) that can be seen from the last plot on Figure 2.

### 3.3 Monte Carlo

We now turn to a Monte Carlo study using the above specified setup and 1,000 replications. Based on the analysis in the previous subsections, the crucial question is how to pick  $R$  as the optimal value of  $R$  depends on the unknown volatility density. From Figure 2 we know that when  $R$  is “too high” for the precision with which we can recover the Laplace transform of volatility from the high-frequency data, then the recovered density starts to oscillate. Therefore, a reasonable and very easy rule is to set  $R$  as the largest value which results with a minimum number of violations

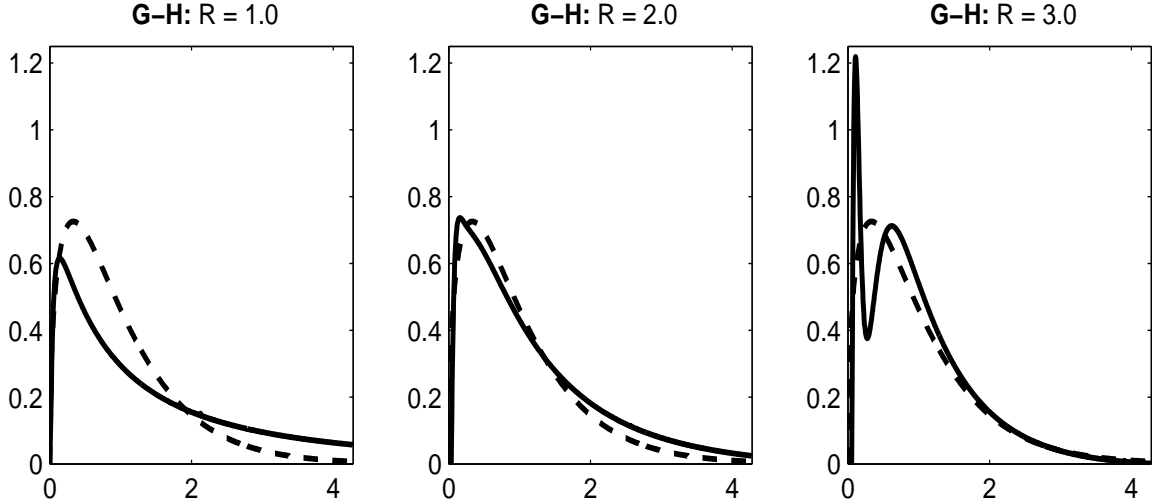


Figure 2: *The effect of regularization.* The figure shows the recovered density of  $V_t$  for a simulated series from model **G-H** whose integrated squared error is reported in Table 3. The solid lines correspond to the estimated density and the dashed lines to the true one.

of the quasiconcavity conditions (see e.g. Koenker and Mizera (2010)) of the recovered volatility density. In particular, for the case plotted in Figure 2, this will lead us to picking the middle value of  $R = 2.0$ .

We implement this rule in the Monte Carlo. We note that this can lead to a different value of  $R$  for the different realizations of the simulated processes. The results from the Monte Carlo are reported in Table 4. As seen from the results in the table, we have relatively good precision with which we can recover the volatility densities across the different simulation scenarios. In general also the mean integrated squared error (MISE) is comparable with the minimal ISE from the single realizations of the process reported in Table 3. The hardest case of all simulation scenarios is the IG-H which corresponds to inverse-Gaussian with very high volatility of volatility. The estimation error involved in this case is relatively big, necessitating small values of  $R$  to attenuate its effect on the inversion, which in turn leads to some bias.

## 4 Empirical Application

We next illustrate the use of the developed nonparametric technique in a short empirical application. We analyze three large-cap stocks that are part of the S&P 100 index: one in the technology sector (IBM), one in utilities and services (Johnson and Johnson, abbreviated by its ticker JNJ) and one in the financial sector (Bank of America, abbreviated by its ticker BAC). The sample period is from April 1997 till December 2010, and we sample every 5-minutes during the trading hours on each

Table 4: Monte Carlo Results: MISE

Case	$\int_{\mathbb{R}} f^2(x)dx$	MISE	Case	$\int_{\mathbb{R}} f^2(x)dx$	MISE
<b>G-L</b>	0.6247	0.0249	<b>IG-L</b>	0.6518	0.0532
<b>G-M</b>	0.5301	0.0184	<b>IG-M</b>	0.5959	0.0321
<b>G-H</b>	0.4765	0.0192	<b>IG-H</b>	0.6911	0.0998

*Note:* The computations are based on 1,000 replica of the models given in Table 1 with  $T = 3,000$  and  $n = 76$ . The MISE is a sample average over the replications of the ISE which in turn is approximated the same way as in the calculations for Table 2. The choice of the regularization parameter  $R$  is over the discrete grid  $1 : 0.25 : 3.5$  and is the largest number of this set with least violations of quasiconcavity of the density estimate.

trading day (which is our unit of time) and this results in 76 high-frequency return observations per day. We exclude days in which there was no trading of the stock for more than half of the day. This resulted in a total of 3423 days for IBM, 3421 for BAC and 3420 days for JNJ in our sample. The 5-minute sampling frequency is coarse enough so that microstructure-noise related issues are of no concern here. Using the truncated variation defined later in (22), we estimate that jumps contribute the nontrivial 11.6, 11.1 and 12.7 percent of the total price variation for IBM, BAC and JNJ stocks respectively.

Before turning to the actual estimation we “standardize” the high-frequency returns, when using them in the calculation of the realized Laplace transform, in order to account for the well-known presence of a diurnal deterministic within-day pattern in volatility, see e.g., Andersen and Bollerslev (1997). To this end,  $V_t$  in (1) is replaced by  $\tilde{V}_t = V_t \times d(t - [t])$  where  $V_t$  is our original stationary volatility process satisfying assumption A and  $d(s)$  is a positive differentiable deterministic function on  $[0, 1]$  that captures the diurnal pattern. Then we standardize each high-frequency increment  $\Delta_i^n X$  with  $1/\sqrt{\hat{d}_i}$  for

$$\hat{d}_i = \frac{\hat{g}_i}{\hat{g}}, \quad \hat{g}_i = \frac{n}{T} \sum_{t=1}^T |\Delta_{i_t}^n X|^2 \mathbf{1}(|\Delta_{i_t}^n X| \leq \alpha n^{-\varpi}), \quad \hat{g} = \frac{1}{n} \sum_{i=1}^n \hat{g}_i, \quad i = 1, \dots, nT, \quad \alpha > 0, \quad \varpi \in (0, 1/2),$$

where  $i_t = t - 1 + i - [i/n]n$ , for  $i = 1, \dots, nT$  and  $t = 1, \dots, T$ . We set  $\varpi = 0.49$  and  $\alpha = 3 \times \sqrt{BV_t}$  for  $BV_t$  denoting the Bipower variation of Barndorff-Nielsen and Shephard (2004, 2006) defined as

$$BV_t = \frac{\pi}{2} \sum_{i=n(t-1)+1}^{nt} |\Delta_{i-1}^n X| |\Delta_i^n X|. \quad (21)$$

Intuitively,  $\hat{d}_i$  estimates the deterministic component of the stochastic variance, and then we “stan-

standardize” the high-frequency increments with it. Todorov and Tauchen (2011) derive the asymptotic effect of this “cleaning” procedure but since  $\widehat{d}_i$  estimates quite precisely the deterministic pattern, naturally this effect is rather small.

We plot the estimated densities of the spot volatility obtained from the estimation method based on the regularized inverse of the realized Laplace transform in (9) for each of the three stocks on the three top panels Figure 3. For ease of interpretation we present the density estimates for  $\sqrt{V_t}$  (and not  $V_t$ ) in percentage terms, as this is the standard way of quoting volatility on the market. We can contrast these spot volatility density estimates with estimates of the density of a jump-robust measure of the daily integrated volatility obtained by inverting its direct empirical Laplace transform. We measure the integrated volatility using the truncated variation, originally proposed in Mancini (2009), and applied here as

$$TV_t = \sum_{i=n(t-1)+1}^{nt} |\Delta_i^n X|^2 \mathbf{1}(|\Delta_{i_t}^n X| \leq \alpha n^{-\varpi}), \quad (22)$$

for the same choice of  $\varpi = 0.49$  and  $\alpha = 3 \times \sqrt{BV_t}$  as for the estimation of the diurnal component of volatility  $\widehat{d}_i$ . Under our assumption A,  $TV_t$  is a consistent estimate for the unobservable integrated volatility (and this is the reason for using it as a benchmark for the volatility density), i.e., we have for each fixed  $t \geq 1$  (see e.g., Jacod (2008))

$$TV_t \xrightarrow{\mathbb{P}} \int_{t-1}^t \sigma_s^2 ds, \quad \text{as } n \rightarrow \infty. \quad (23)$$

The dashed lines in the top three panels of Figure 3 show the implied density for the daily integrated volatility from using our method to invert the empirical Laplace transform of the  $\sqrt{TV_t}$  series, while the three lower panels show standard kernel-density estimates of  $\sqrt{TV_t}$  obtained from the same observations.

There are several conclusions to be made from Figure 3. First, there is significant volatility of volatility: the spot volatility can take values as high as five to six times its modal value. Thus volatility dynamics (and in particular short-lived sharp changes in it) play an important role in generating tail events in individual stock returns in addition to the price jumps. We recall that the realized Laplace transform is robust to presence of price jumps. Therefore our nonparametric separation of volatility from jumps identifies a rather nontrivial role of stochastic volatility for generating extreme events in asset prices. Not surprisingly IBM (being the most diversified of the three stocks) has lowest variance while BAC has the highest. Comparing the spot with integrated volatility we can see a common pattern in the three stocks. The mode of the spot volatility density is slightly to the left of that for the daily integrated volatility, and spot volatility has somewhat fatter

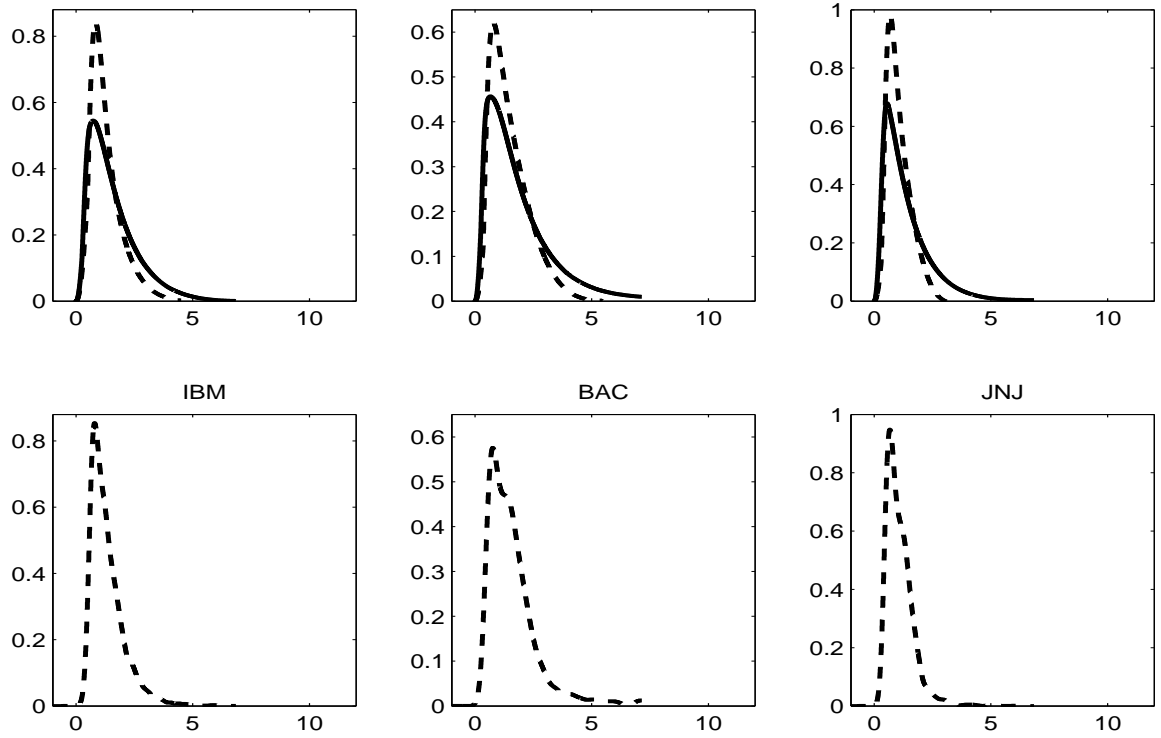


Figure 3: *Nonparametric Spot and Integrated Volatility Density Estimates.* The solid lines correspond to our nonparametric estimate for the density of  $\sqrt{V_t}$  while the dashed lines are nonparametric density estimates of daily  $\sqrt{TV_t}$ . The dashed lines in the top plots are based on inverting the empirical Laplace transform of  $TV_t$  using our estimator in (9) while the ones in the bottom plots are standard kernel estimates with Silverman's automatic bandwidth of  $h = 0.79 \times \text{IQR} \times T^{-1/5}$  for IQR denoting the inter-quartile range.

distribution than that of the integrated volatility. The reason for this is in the presence of short term volatility moves in the form of volatility jumps and the mean reversion. The daily integrated volatility “averages out” the sharp moves in volatility. Overall our nonparametric evidence here points to stochastic volatility with significant volatility of volatility possibly generated by volatility jumps.

We investigate further the hypothesis of volatility jumps and their interaction with the price jumps by computing conditional density estimates. In particular, we will use the methodology developed here to gather nonparametric evidence regarding the effect of price jumps on stochastic volatility. In standard volatility models, volatility is a diffusion process and thus by construction stochastic volatility is independent from the price jumps. More recent parametric work has allowed for volatility jumps as in the non-Gaussian OU model of Barndorff-Nielsen and Shephard (2001), although in some specifications volatility and price jumps are constrained to be uncorrelated.

To investigate the effect of price jumps on volatility we do the following. We identify the days in the sample where relatively large jumps occurred (we will be precise about what constitutes a large jump below) and then construct the realized Laplace transform of volatility on a given (fixed) number of days after the day with the large jump. We then use our nonparametric procedure to invert the estimated Laplace transform and recover the density of volatility a fixed number of days after the occurrence of price jumps. More formally, for some “big” fixed  $\tau > 0$  we define for any integer  $k \geq 1$  the set of days with a “big” positive, respectively negative, jump as

$$I_n^{\pm\tau}(k) = \left\{ t = k + 1, \dots, T : \{i = (t - k - 1)n + 1, \dots, (t - k)n\} \cap \{i = 1, \dots, nT : \Delta_i^n X \geq \pm(\alpha n^{-\varpi} \vee \tau)\} \neq \emptyset \right\},$$

where  $\alpha$  and  $\varpi$  are the same as the ones used in the construction of  $TV_t$ .  $I_n^{\pm\tau}(k)$  is the set of days in the sample where  $k$  days ago a big positive or negative jump has occurred. We can then construct the realized Laplace transform on the sets  $I_n^{\pm\tau}(k)$ , i.e.,

$$\widehat{\mathcal{L}}^{\pm\tau}(k) = \frac{1}{|I_n^{\pm\tau}(k)|} \sum_{t \in I_n^{\pm\tau}(k)} \left[ \sum_{i=(t-1)n+1}^{tn} \cos\left(\sqrt{2un}\Delta_i^n X\right) \right], \quad (24)$$

where  $|I_n^{\pm\tau}(k)|$  denotes the size of the set  $I_n^{\pm\tau}(k)$ . Finally, we can invert  $\widehat{\mathcal{L}}^{\pm\tau}(k)$  using (9). Our goal is to produce a nonparametric estimate of the densities of  $\sqrt{V_t}1_{\{t \in I^{-\tau}(k)\}}$  and  $\sqrt{V_t}1_{\{t \in I^{+\tau}(k)\}}$  where the set  $I^{\pm\tau}(k)$  is defined via

$$I^{\pm\tau}(k) = \left\{ t : \llbracket t \rrbracket - k - 1; \llbracket t \rrbracket - k \right\} \cap \{s > 0 : \Delta X_s \geq \pm\tau\} \neq \emptyset. \quad (25)$$

In our actual application we set  $\tau$  to  $\tau = \sqrt{\mathbb{E}(TV_t)} \times 5/\sqrt{n}$  which is five-standard deviation move for the continuous part of the high-frequency return (the mean of the truncated variation is estimated

by the corresponding sample average). This results in approximately 100 jumps of each sign in our sample to estimate the realized Laplace transforms in (24). We further set  $k$  to 1 and 22 which amounts to looking at volatility 1 day and 1 calendar month after a “big” jump.

The result of the calculations are presented on Figure 4. There are several interesting common patterns across the three stocks. First, comparing the estimated volatility densities on Figure 4 with the unconditional ones on Figure 3 we can see a very pronounced shift of the mode towards the right, i.e., volatility unambiguously increases after a “big” jump. Interestingly, the density of the volatility one month after the jump starts moving towards the unconditional one (compared with the density the day following the jump). The interpretation is that a big price jump “feeds” into higher future volatility with the effect slowly diminishing over time due to the mean reversion in volatility. This shows that price jumps are very closely related with the stochastic volatility dynamics and in particular in terms of parametric volatility modeling we need models that allow for this connection as for example in the non-Gaussian OU model of Barndorff-Nielsen and Shephard (2001). Another interesting common pattern across the three stocks is that there is a significant spread in the estimated volatility densities on Figure 4. This suggests that the size of the price jumps plays a big role in determining the size of the impact it has on the future stochastic volatility. Thus the connection between volatility and price jumps is size dependent. Further, comparing the left and the right side of Figure 4 we can see that the volatility densities after a positive and a negative jump are rather similar for these three stocks. Finally, it is interesting to point out that among the three stocks, the one whose volatility reacts strongest to the occurrence of price jumps is BAC. This is consistent with the view that stocks in the financial sector are most sensitive to financial distress in the form of extreme market events, i.e., jumps.

## 5 Conclusion

In this paper we propose a nonparametric method for estimation of the spot volatility density in a jump-diffusion model from high-frequency data with increasing time span. The method consists of aggregating the high-frequency returns data into a function known as realized Laplace transform, which provides a consistent estimate of the unobservable real-valued volatility Laplace transform. On a second stage the estimated volatility Laplace transform is inverted using a regularized kernel method to obtain an estimate of the density of spot volatility. We derive bounds on the MISE in the density estimation and provide guidance on the feasible choice of the regularization parameter. An empirical application for three large-cap stocks indicates the importance of short-term high frequency movements in volatility that get smoothed over in forming estimates of daily realized

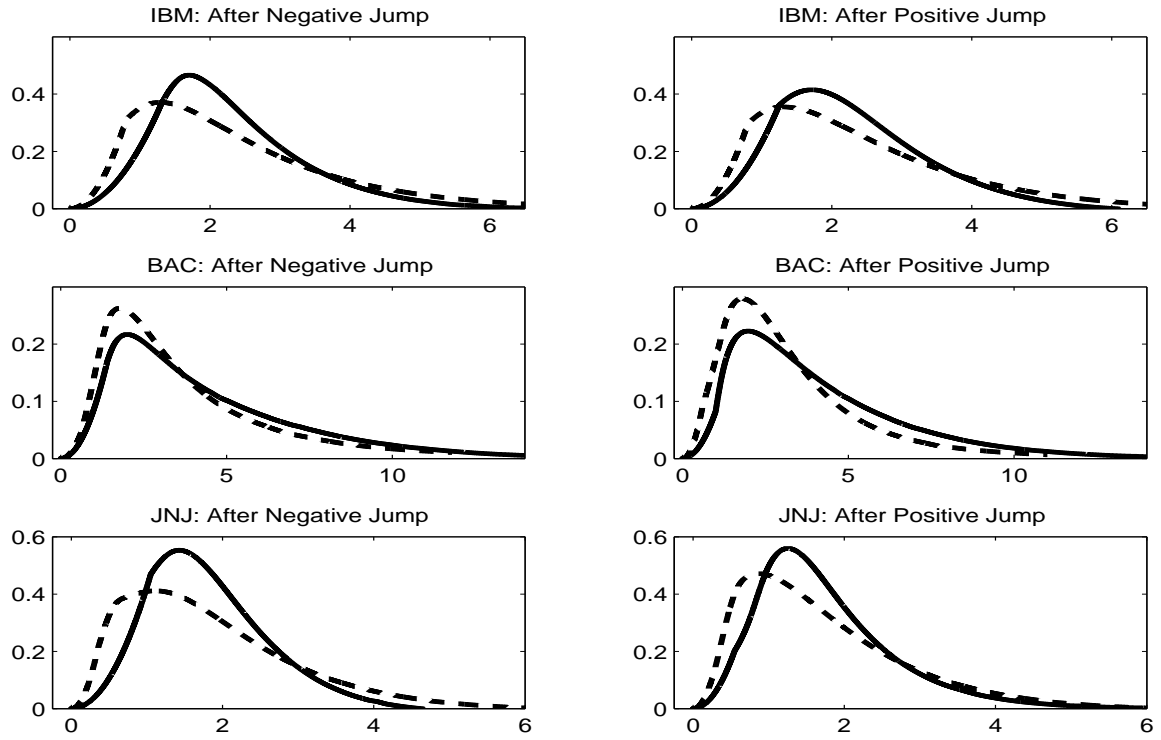


Figure 4: *Nonparametric Volatility Density Estimates After a Price Jump.* The solid (dashed) line is a nonparametric density estimate of  $\sqrt{V_t}$  over the days in the sample which follow a day (respectively 22 days) after a positive (left side) or negative “big” jump (right side) in the price. The threshold for the “big” jumps is set to five standard deviations of the continuous part of the high-frequency return based on the sample mean of  $TV_t$  of each individual series.

variation, and it shows how to trace out the dynamic response of the spot volatility density to large price jumps of either sign as it relaxes back to the steady state unconditional density.

## 6 Proofs

The proof of Theorem 1 consists of two parts. The first part is analysis of the deterministic bias  $f_R(x) - f(x)$  (respectively  $\int_{\mathbb{R}} (f_R(x) - f(x))^2 dx$ ) and the second part deals with the estimation error  $\widehat{f}_R(x) - f_R(x)$  (respectively  $\int_{\mathbb{R}} w(x)(\widehat{f}_R(x) - f_R(x))^2 dx$  and  $\int_{\mathbb{R}} (\widehat{f}_R(x) - f_R(x))^2 dx$ ). In what follows we will denote with  $K$  a positive constant that does not depend on  $R$ ,  $x$ ,  $T$  and  $n$ .

### 6.1 The deterministic bias $f_R(x) - f(x)$

Using the representation of  $f_R(x)$  in Kryzhniy (2003a) as an integral with respect to the true density  $f(x)$ , we have

$$\begin{aligned} f_R(x) &= \frac{2 \coth(\pi R)}{\pi} \int_0^\infty f(xu) \sqrt{u} \frac{\sin(R \ln(u))}{u^2 - 1} du = \frac{2 \coth(\pi R)}{\pi} \int_{-\infty}^\infty f(xe^z) e^{3z/2} \frac{\sin(Rz)}{e^{2z} - 1} dz \\ &= \frac{2}{\pi} \int_{-\infty}^\infty f(xe^z) e^{3z/2} \frac{\sin(Rz)}{e^{2z} - 1} dz + O(e^{-2\pi R}). \end{aligned} \quad (26)$$

Using the above, we can make the decomposition (recall the definition of  $\widetilde{f}(x)$  in the theorem) for some constant  $\delta > 1/R$

$$\begin{aligned} f_R(x) - \widetilde{f}(x) &= \sum_{i=1}^4 A_i(x) + O(e^{-2\pi R}), \quad (27) \\ A_1(x) &= \frac{2}{\pi} \int_{-\delta}^0 [f(xe^z) - f(x-)] \frac{e^{3z/2} \sin(Rz)}{e^{2z} - 1} dz + \frac{2}{\pi} \int_0^\delta [f(xe^z) - f(x+)] \frac{e^{3z/2} \sin(Rz)}{e^{2z} - 1} dz, \\ A_2(x) &= \frac{2}{\pi} \int_{-\infty}^{-\delta} [f(xe^z) - f(x-)] \frac{e^{3z/2} \sin(Rz)}{e^{2z} - 1} dz, \quad A_3(x) = \frac{2}{\pi} \int_\delta^\infty [f(xe^z) - f(x+)] \frac{e^{3z/2} \sin(Rz)}{e^{2z} - 1} dz, \\ A_4(x) &= f(x-) \left( \frac{1}{\pi} \int_{-\infty}^0 \frac{e^{z/2} \sin(Rz)}{\sinh(z)} dz - \frac{1}{2} \right) + f(x+) \left( \frac{1}{\pi} \int_0^\infty \frac{e^{z/2} \sin(Rz)}{\sinh(z)} dz - \frac{1}{2} \right). \end{aligned}$$

Starting with  $A_1(x)$ , we can split the range of integration  $(-\delta, 0)$  to  $(-\delta, -1/R)$  and  $(-1/R, 0)$  (and similarly for the positive side) and we use different arguments to bound each of the integrals. First, since  $f(x)$  is piecewise differentiable, we can apply Taylor expansion and trivially get

$$\begin{aligned} &\left| \int_{-1/R}^0 [f(xe^z) - f(x-)] \frac{e^{3z/2} \sin(Rz)}{e^{2z} - 1} dz \right| + \left| \int_0^{1/R} [f(xe^z) - f(x+)] \frac{e^{3z/2} \sin(Rz)}{e^{2z} - 1} dz \right| \\ &\leq \sup_{u \in [e^{-1/R}x, e^{1/R}x]} |f'(u)u| \frac{K}{R}. \end{aligned} \quad (28)$$

Next, using integration by parts, we have

$$\int_{-\delta}^{-1/R} [f(xe^z) - f(x-)] \frac{e^{3z/2} \sin(Rz)}{e^{2z} - 1} dz = \frac{1}{R} \int_{-\delta}^{-1/R} g'(z) \cos(Rz) dz - \frac{1}{R} (g(-1/R) \cos(-1) - g(-\delta) \cos(-R\delta)), \quad (29)$$

where  $g(z) = \frac{(f(xe^z) - f(x-))e^{3z/2}}{e^{2z} - 1}$  and  $g'(z)$  is its derivative. Using the fact that  $f(x)$  has a piecewise continuous derivative, we get that

$$|g(-1/R)| + |g(-\delta)| \leq K \sup_{u \in [e^{-\delta}x, x]} |f'(u)u|. \quad (30)$$

We further have

$$g'(z) = \frac{f'(xe^z)xe^{5z/2}}{e^{2z} - 1} + \frac{1.5e^{3z/2} [f(xe^z) - f(x-)]}{e^{2z} - 1} - \frac{2e^{7z/2} [f(xe^z) - f(x-)]}{(e^{2z} - 1)^2},$$

from which it follows

$$|g'(z)| \leq K \sup_{u \in [e^{-\delta}x, x]} |f'(u)u| \frac{1}{1 - e^z}, \quad z \in (-\delta, -1/R). \quad (31)$$

Therefore,  $\int_{-\delta}^{-1/R} g'(z) \cos(Rz) dz = O(\log(R))$  for a given  $x > 0$ . Similar analysis of course can be made on the interval  $(1/R, \delta)$ , and thus altogether we have

$$A_1(x) = O\left(\frac{\log(R)}{R}\right), \quad \forall x > 0. \quad (32)$$

We continue next with  $A_2(x)$ . We can decompose it as

$$A_2(x) = \frac{2}{\pi} [A_2^{(1)}(x) + A_2^{(2)}(x) - A_2^{(3)}(x)], \quad A_2^{(1)}(x) = \int_{-\infty}^{-\delta - \lfloor \frac{R \log(R)}{3\pi} \rfloor \frac{2\pi}{R}} f(xe^z) e^{3z/2} \frac{\sin(Rz)}{e^{2z} - 1} dz, \\ A_2^{(2)}(x) = \int_{-\delta - \lfloor \frac{R \log(R)}{3\pi} \rfloor \frac{2\pi}{R}}^{-\delta} f(xe^z) e^{3z/2} \frac{\sin(Rz)}{e^{2z} - 1} dz, \quad A_2^{(3)}(x) = f(x-) \int_{-\infty}^{-\delta} e^{3z/2} \frac{\sin(Rz)}{e^{2z} - 1} dz.$$

First, using the behavior of  $f(x)$  around zero from assumption B1 (and the identity  $f(y) = f(x) + \int_x^y f'(u) du$  for each interval  $[x, y]$  on which  $f(u)$  and  $f'(u)$  are continuous), we trivially have

$$A_2^{(1)}(x) = O\left(R^{-(5/3 - 2q/3) \wedge 1}\right), \quad \forall x > 0, \quad (33)$$

for  $q$  being the the constant in assumption B1. We further have

$$A_2^{(2)}(x) = \sum_{k=1}^{\lfloor \frac{R \log(R)}{3\pi} \rfloor} h(-\delta - 2\pi k/R) \int_{-\delta - 2\pi k/R}^{-\delta - 2\pi(k-1)/R} e^{3z/2} \sin(Rz) dz \\ + \sum_{k=1}^{\lfloor \frac{R \log(R)}{3\pi} \rfloor} \int_{-\delta - 2\pi k/R}^{-\delta - 2\pi(k-1)/R} (h(z) - h(-\delta - 2\pi k/R)) e^{3z/2} \sin(Rz) dz, \quad (34)$$

where we denote  $h(z) = \frac{f(xe^z)}{e^{2z}-1}$ . Using assumption B1, we have  $|h(z)|/e^{-z((q-1)\vee 0)} \leq K(x)$  for  $z$  sufficiently small (and fixed  $x$ ). Therefore, using direct integration, we have for every  $x > 0$

$$\sum_{k=1}^{\lfloor \frac{R \log(R)}{3\pi} \rfloor} h(-\delta - 2\pi k/R) \int_{-\delta-2\pi k/R}^{-\delta-2\pi(k-1)/R} e^{3z/2} \sin(Rz) dz = O(R^{-(5/3-2q/3)\wedge 1} \times \log(R) 1_{\{q \leq 1\}}).$$

Similarly, using  $|h'(z)|/e^{-z((q-1)\vee 0)} \leq K(x)$  for  $z$  sufficiently small (and fixed  $x$ ), we have for every  $x > 0$

$$\begin{aligned} \sum_{k=1}^{\lfloor \frac{R \log(R)}{3\pi} \rfloor} \int_{-\delta-2\pi k/R}^{-\delta-2\pi(k-1)/R} (h(z) - h(-\delta - 2\pi k/R)) e^{3z/2} \sin(Rz) dz \\ = O(R^{-(5/3-2q/3)\wedge 1} \times \log(R) 1_{\{q \leq 1\}}). \end{aligned}$$

Thus altogether we have

$$A_2^{(2)}(x) = O\left(R^{-(5/3-2q/3)\wedge 1} \times \log(R) 1_{\{q \leq 1\}}\right), \quad \forall x > 0. \quad (35)$$

Finally, using integration by parts it is easy to show

$$A_2^{(3)}(x) = O(1/R), \quad \forall x > 0. \quad (36)$$

Similar analysis can be made of course for  $A_3(x)$ , and thus altogether we have

$$|A_2(x)| + |A_3(x)| = O\left(R^{-(5/3-2q/3)\wedge 1} \times \log(R) 1_{\{q \leq 1\}}\right), \quad \forall x > 0. \quad (37)$$

We are left with  $A_4(x)$ . We can write

$$\begin{aligned} A_4(x) &= \frac{f(x-)}{\pi} \int_{-\infty}^0 \frac{(e^{z/2} - 1) \sin(Rz)}{\sinh(z)} dz + \frac{f(x+)}{\pi} \int_0^{\infty} \frac{(e^{z/2} - 1) \sin(Rz)}{\sinh(z)} dz \\ &\quad + \tilde{f}(x) \left( \frac{1}{\pi} \int_0^{\infty} \frac{\sin(Rz)}{\sinh(z)} dz - \frac{1}{2} \right). \end{aligned} \quad (38)$$

Using integration by parts for the first two integrals on the right side of the above equality and the identity  $\int_0^{\infty} \frac{\sin(Rz)}{\sinh(z)} dz = \frac{\pi}{2} \tanh\left(\frac{\pi R}{2}\right)$  for the third one, we trivially get

$$A_4(x) = O(1/R), \quad \forall x > 0. \quad (39)$$

Combining the results in (32), (37) and (39) we have the second claim in (10).

For the claim in (12) we will show here that

$$\int_0^{\infty} (f_R(x) - f(x))^2 dx = O\left(\frac{\log^2(R)}{R^2}\right). \quad (40)$$

For this it suffices to show

$$\int_0^\infty (\phi_R(x) - f(x))^2 dx = O\left(\frac{\log^2(R)}{R^2}\right), \quad (41)$$

where  $\phi_R(x) = \frac{2}{\pi} \int_{-\infty}^\infty f(xe^z) e^{3z/2} \frac{\sin(Rz)}{e^{2z}-1} dz$ . This follows from the inequality

$$\int_0^\infty \phi_R^2(x) dx \leq 2 \int_0^\infty f^2(x) dx + 2 \int_0^\infty (\phi_R(x) - f(x))^2 dx,$$

the decomposition in (26), and since  $f(x) \in L^2(\mathbb{R})$  by assumption B2.

We make the decomposition of  $\phi_R(x) - f(x) = \sum_{i=1}^4 A_i(x)$ . Then using the bounds in (28), (30), (31) and (38) and assumption B2, we have

$$\int_0^\infty (A_1^2(x) + A_4^2(x)) dx = O\left(\frac{\log^2(R)}{R^2}\right). \quad (42)$$

For the two terms  $A_2(x)$  and  $A_3(x)$  we use a different decomposition than the one we used above for showing (10). In particular, we now decompose  $A_2(x)$  using integration by parts as

$$A_2(x) = \frac{1}{R} \int_{-\infty}^{-\delta} g'(z) \cos(Rz) dz - \frac{1}{R} (g(-\delta) \cos(-R\delta) - g(-\infty) \cos(-\infty)),$$

where recall we denote  $g(z) = \frac{[f(xe^z) - f(x-)]e^{3z/2}}{e^{2z}-1}$  and  $g'(z)$  is its derivative, and we do exactly the same decomposition for  $A_3(x)$ . Then using the boundedness of  $f(x)$  as well as  $f'(x)$  with  $f(x) = o(x^{-1-\iota})$  and  $f'(x) = o(x^{-2-\iota})$  for  $x \rightarrow \infty$  together with Fubini's theorem (integrating first over  $x$ ), we can easily get

$$\int_0^\infty (A_2^2(x) + A_3^2(x)) dx = O\left(\frac{\log^2(R)}{R^2}\right). \quad (43)$$

Finally, for the deterministic bias component of the bound in (14), we can use directly (40) combined with

$$\int_0^\infty (\chi(R^2 x) - 1)^2 dx \leq K/R^2,$$

to get

$$\int_0^\infty (\tilde{f}_R(x) - f(x))^2 dx = O\left(\frac{\log^2(R)}{R^2}\right). \quad (44)$$

## 6.2 The estimation error $\widehat{f}_R(x) - f_R(x)$

We first decompose the error in estimating the volatility Laplace transform as follows

$$\begin{aligned} \widehat{\mathcal{L}}(u) - \mathcal{L}(u) &= B_1(u) + B_2(u) + B_3(u) + B_4(u) + B_5(u), \\ B_1(u) &= \frac{1}{T} \int_0^T (e^{-uV_s} - \mathcal{L}(u)) ds, \quad B_2(u) = \frac{1}{T} \int_0^T (e^{-uV_{\lfloor sn \rfloor/n}} - e^{-uV_s}) ds, \end{aligned}$$

$$\begin{aligned}
B_3(u) &= \frac{1}{nT} \sum_{i=1}^{nT} \left( \cos \left( \sqrt{2un} \Delta_i^n X \right) - \cos \left( \sqrt{2un} \int_{\frac{i-1}{n}}^{\frac{i}{n}} \sqrt{V_s} dW_s \right) \right), \\
B_4(u) &= \frac{1}{nT} \sum_{i=1}^{nT} \left( \cos \left( \sqrt{2un} \int_{\frac{i-1}{n}}^{\frac{i}{n}} \sqrt{V_s} dW_s \right) - \cos \left( \sqrt{2un} \sqrt{V_{\frac{i-1}{n}}} \Delta_i^n W \right) \right), \\
B_5(u) &= \frac{1}{nT} \sum_{i=1}^{nT} \left( \cos \left( \sqrt{2un} \sqrt{V_{\frac{i-1}{n}}} \Delta_i^n W \right) - e^{uV_{\lfloor sn \rfloor / n}} \right).
\end{aligned}$$

Starting with the first term, we can apply Lemma VIII.3.102 in Jacod and Shiryaev (2003) and our assumption A4, and get

$$\mathbb{E}(B_1(u)) = 0 \quad \text{and} \quad \mathbb{E}|B_1(u)|^2 \leq \frac{K(u)}{T} \int_0^\infty \alpha_s^{\text{mix}} ds, \quad (45)$$

where the positive  $K(u)$  depends only on  $u$  and further  $K(u) = o(u^{-\alpha})$  as  $u \rightarrow \infty$  for some  $\alpha > 0$ . We note that  $\int_0^\infty \alpha_s^{\text{mix}} ds$  is finite due to our assumption on the rate of decay of the mixing coefficients in assumption A4.

We continue next with  $B_2(u)$ . First, using Taylor expansion we can get the inequality  $|e^{-x^p} - e^{-y^p}| \leq K|x - y|$  for  $x, y \in \mathbb{R}_+$  and some constant  $K$  and  $p \geq 1$ . Then using the classical inequality

$$||x|^r - |y|^r| \leq |x - y|^r, \quad \text{for some } r \in (0, 1],$$

we can get  $|e^{-x} - e^{-y}| \leq K|x - y|^r$  for  $x, y \in \mathbb{R}_+$  and any  $r \leq 1$ . Applying the last inequality with  $x = V_{\lfloor sn \rfloor / n}$  and  $y = V_s$ , and then using assumption A3, together with Lemma VIII.3.102 in Jacod and Shiryaev (2003) and our assumption A4, we get

$$\begin{aligned}
\mathbb{E}|B_2(u)|^2 &= \frac{1}{T^2} \mathbb{E} \left\{ \int_0^T \int_0^T (e^{-uV_{\lfloor tn \rfloor / n}} - e^{-uV_t}) (e^{-uV_{\lfloor sn \rfloor / n}} - e^{-uV_s}) ds dt \right\} \\
&\leq \frac{Ku^{1-\iota} n^{-1/2+\iota}}{T^2} \int_0^T \int_0^T \left( \alpha_{|t-s|^{-1/n}}^{\text{mix}} \right) dt ds \leq \frac{Ku^{1-\iota} n^{-1/2+\iota}}{T},
\end{aligned}$$

for  $\iota > 0$  arbitrary small. From here we have altogether

$$\mathbb{E}|B_2(u)| \leq \frac{Ku^{1/2-\iota} n^{-1/4+\iota}}{\sqrt{T}} \quad \text{and} \quad \mathbb{E}|B_2(u)|^2 \leq \frac{Ku^{1-\iota} n^{-1/2+\iota}}{T}, \quad \forall \iota > 0. \quad (46)$$

Next, using the trigonometric identities for  $\cos(a) - \cos(b)$  and  $\sin(a+b)$ , the fact that  $|\sin(x)| \leq |x|$ , as well as the Hölder inequality (together with assumptions A1 and A3) and Burkholder-Davis-Gundy inequality, we get for  $B_3(u)$

$$\mathbb{E}|B_3(u)| \leq Ku^{1/2-\iota} n^{[\beta/2-1 \wedge (1/\beta)+\iota] \vee (-1/2)} \quad \text{and} \quad \mathbb{E}|B_3(u)|^2 \leq Ku^{1-\iota} n^{\beta/2-1+\iota}, \quad (47)$$

where  $\iota > 0$  is arbitrary small. Turning to  $B_4(u)$ , we can distinguish two cases: when assumption B1 holds and when the stronger B2 holds. In the case of B1 only, we can use Itô isometry and Hölder inequality to get

$$\mathbb{E}|B_4(u)| \leq Ku^{1/2-\iota}n^{-1/4+\iota} \quad \text{and} \quad \mathbb{E}|B_4(u)|^2 \leq Ku^{1-\iota}n^{-1/2+\iota}, \quad \forall \iota > 0, \quad \text{under B1.} \quad (48)$$

When the stronger condition B2 holds, we can make use of the following identity

$$\sqrt{x} - \sqrt{y} = \frac{1}{2\sqrt{x}}(x - y) + \frac{(\sqrt{x} - \sqrt{y})^2}{2\sqrt{x}}, \quad \forall x > 0, y \geq 0.$$

Applying the above, together with Itô isometry, Holder's inequality, the fact that  $f(x) \leq Kx$  for  $x$  around zero (because of the boundedness of  $f'(x)$  and  $f(0+) = 0$ ) which implies that  $\mathbb{E}|V_t|^{\iota-2} \leq K$  for any  $\iota > 0$ , as well as assumption A3, we can get the stronger bound

$$\mathbb{E}|B_4(u)| \leq Ku^{1/2-\iota}n^{-1/2+\iota} \quad \text{and} \quad \mathbb{E}|B_4(u)|^2 \leq Ku^{1-\iota}n^{-1+\iota}, \quad \forall \iota > 0, \quad \text{under B2.} \quad (49)$$

Finally, for  $B_5(u)$ , we can use successive conditioning and get

$$\mathbb{E}(B_5(u)) = 0 \quad \text{and} \quad \mathbb{E}(B_5(u))^2 \leq \frac{K}{nT}. \quad (50)$$

Now we are ready to show the result in (11) and its equivalent for the integrated squared error.

We have

$$\widehat{f}_R(x) - f_R(x) = \int_{\mathbb{R}_+} \Pi(R, xu) \left( \widehat{\mathcal{L}}(u) - \mathcal{L}(u) \right) du.$$

Using integration by parts twice, we have for  $x > 0$

$$\begin{aligned} \int_0^\infty \frac{\sqrt{u} \sin(R \ln(u))}{u^2 + 1} \sin(xu) du &= \frac{1}{x^2} \int_0^\infty \sin(xu) \Xi(u, R) du, \\ \Xi(u, R) &= -\frac{0.25u^{-3/2} \sin(R \ln(u))}{u^2 + 1} - \frac{u^{-3/2} \sin(R \ln(u))}{(u^2 + 1)^{3/2}} - \frac{3u^{1/2} \sin(R \ln(u))}{(u^2 + 1)^2} + \frac{4u^{5/2} \sin(R \ln(u))}{(u^2 + 1)^3} \\ &\quad - \frac{4Ru^{1/2} \cos(R \ln(u))}{(u^2 + 1)^2} - \frac{R^2u^{-3/2} \sin(R \ln(u))}{u^2 + 1}. \end{aligned}$$

From here, using the identity  $|\sin(x)/x| \leq 1$ , we have  $\left| \int_0^\infty \frac{\sqrt{u} \sin(R \ln(u))}{u^2 + 1} \sin(xu) du \right| \leq KR^2(x^{1/2-\iota} \wedge x^{-3/2+\iota})$  (for the first part of this bound we do not need the above decomposition but only the inequality  $|\sin(x)/x| \leq 1$ ) for any  $\iota > 0$ . Similar results holds for  $\int_0^\infty \frac{\sqrt{u} \cos(R \ln(u))}{u^2 + 1} \sin(xu) du$  as well and we thus have  $|\Pi(R, z)| \leq e^{\pi R} R^2 \widehat{\Pi}(z)$  for some  $\widehat{\Pi}(z)$  with  $\widehat{\Pi}(z) = o(z^{1/2-\iota})$  for  $z \rightarrow 0$  and  $\widehat{\Pi}(z) = o(z^{-3/2+\iota})$  for  $z \rightarrow \infty$  and arbitrary small  $\iota > 0$ . From here an application of Fubini's theorem, together with the results in (45), (46), (47), (48), (49) and (50), yields

$$\begin{aligned} \mathbb{E} \left\{ \int_0^\infty \int_0^\infty \int_0^\infty w^2(x) \Pi(R, xu) \Pi(R, xv) |\widehat{\mathcal{L}}(u) - \mathcal{L}(u)| |\widehat{\mathcal{L}}(v) - \mathcal{L}(v)| dudvdx \right\} \\ \leq Ke^{\pi R} R^4 \left( T^{-1} + n^{-1+\beta/2+\iota} \right) \int_0^\infty \frac{w^2(x)}{x^{3-\iota}} dx \leq Ke^{\pi R} R^4 \left( T^{-1} + n^{-1+\beta/2+\iota} \right), \end{aligned}$$

$$\mathbb{E} \left\{ \int_0^\infty \int_0^\infty \int_0^\infty \chi^2(R^2x) \Pi(R, xu) \Pi(R, xv) |\widehat{\mathcal{L}}(u) - \mathcal{L}(u)| |\widehat{\mathcal{L}}(v) - \mathcal{L}(v)| dudvdx \right\} \\ \leq Ke^{\pi R} R^4 \left( T^{-1} + n^{-1+\beta/2+\iota} \right) \int_0^\infty \frac{\chi^2(R^2x)}{x^{3-\iota}} dx \leq Ke^{\pi R} R^8 \left( T^{-1} + n^{-1+\beta/2+\iota} \right).$$

From here the rate in (11) as well as their analogues for the integrated squared estimation error in (12) and (14) follow.  $\square$

## References

- Andersen, T., T. Bollerslev, F. Diebold, and P. Labys (2001). The Distribution of Realized Exchange Rate Volatility. *Journal of the American Statistical Association* 96, 42–55.
- Andersen, T. G. and T. Bollerslev (1997). Intraday Periodicity and Volatility Persistence in Financial Markets. *Journal of Empirical Finance* 4, 115–158.
- Barndorff-Nielsen, O. and N. Shephard (2001). Non-Gaussian Ornstein–Uhlenbeck-Based Models and some of Their Uses in Financial Economics. *Journal of the Royal Statistical Society Series B*, 63, 167–241.
- Barndorff-Nielsen, O. and N. Shephard (2004). Power and Bipower Variation with Stochastic Volatility and Jumps. *Journal of Financial Econometrics* 2, 1–37.
- Barndorff-Nielsen, O. and N. Shephard (2006). Econometrics of Testing for Jumps in Financial Economics using Bipower Variation. *Journal of Financial Econometrics* 4, 1–30.
- Black, F. (1976). Studies of stock price volatility changes. *Proceedings of the Business and Economics Section of the American Statistical Association*, 177–181.
- Bollerslev, T. and V. Todorov (2011). Estimation of Jump Tails. *Economtrica*, forthcoming.
- Comte, F. and V. Genon-Catalot (2006). Penalized Projection Estimator for Volatility Density. *Scandinavian Journal of Statistics* 33, 875–893.
- Fan, J. (1991). On the Optimal Rates of Convergence for Nonparametric Deconvolution Problems. *Annals of Statistics* 19, 1257–1272.
- Feller, W. (1971). *An Introduction to Probability Theory and Its Applications*. Volume II. John Wiley.
- Jacod, J. (2008). Asymptotic Properties of Power Variations and Associated Functionals of Semimartingales. *Stochastic Processes and their Applications* 118, 517–559.
- Jacod, J. and A. N. Shiryaev (2003). *Limit Theorems For Stochastic Processes* (2nd ed.). Berlin: Springer-Verlag.
- Klüppelberg, C., A. Lindner, and R. Maller (2004). A Continuous Time GARCH Process Driven by a Lévy Process: Stationarity and Second Order Behavior. *Journal of Applied Probability* 41, 601–622.
- Koenker, R. and I. Mizera (2010). Quasi-concave density estimation. *The Annals of Statistics* 38, 2998–3027.
- Kryzhniy, V. (2003a). Direct Regularization of the Inversion of Real-Valued Laplace Transforms. *Inverse Problems* 19, 573–583.
- Kryzhniy, V. (2003b). Regularized Inversion of Integral Transformations of Mellin Convolution Type. *Inverse Problems* 19, 1227–1240.

- Mancini, C. (2009). Non-parametric Threshold Estimation for Models with Stochastic Diffusion Coefficient and Jumps. *Scandinavian Journal of Statistics* 36, 270–296.
- Mykland, P. and L. Zhang (2009). Inference for Continuous Semimartingales Observed at High Frequency. *Econometrica* 77, 1403–1445.
- Prakasa Rao, B. (1988). Statistical Inference from Sampled Data for Stochastic Processes. In *Contemporary Mathematics*, Volume 80. Amer. Math. Soc., Providence.
- Sato, K. (1999). *Lévy Processes and Infinitely Divisible Distributions*. Cambridge, UK: Cambridge University Press.
- Tikhonov, A. and V. Arsenin (1977). *Solutions of Ill-Posed Problems*. Washington: Winston.
- Todorov, V. and G. Tauchen (2011). The Realized Laplace Transform of Volatility. *Econometrica*, forthcoming.
- Todorov, V., G. Tauchen, and I. Gryniv (2011). Realized Laplace Transforms for Estimation of Jump-Diffusive Volatility Models. *Journal of Econometrics* 164, 367–381.
- Van Es, B., P. Spreij, and H. Van Zanten (2003). Nonparametric Volatility Density Estimation. *Bernoulli* 9, 451–465.